Prepublished copy

Nature Environment & Pollution Technology

This is a peer-reviewed prepublished version of the paper to be published in Vol. 25, No. 3, September 2026 issue

ANN-Driven Optimization of VOC Adsorption on Activated Carbon with Thermal Breakthrough Forecasting and IoT-Based Real-Time Monitoring

Subramanian Kavitha[1]†, Subramani Umamaheswari[2], Venkatesh Babu Samikannu[3], Surendran Ganesan[4]

[1]Department of Chemical Engineering, Hindusthan College of Engineering and Technology, Coimbatore, T.N., India

[2]Department of Science and Humanities, Dhaanish Ahmed Institute of Technology, Coimbatore, T.N., India

[3]Department of Petroleum Engineering, JCT College of Engineering and Technology, Coimbatore, India

[4]Department of Chemical Engineering, KPR Institute of Engineering and Technology, Coimbatore, T.N., India

†Corresponding author: S.Kavitha; kavitha212418@gmail.com

ORCID DETAILS OF THE AUTHORS

Subramanian Kavitha: https://orcid.org/ 0000- 0002-2851-8093

Subramani Umamaheswari : https://orcid.org/0009- 0008-7735-0726

Venkatesh Babu Samikannu: https://orcid.org/0000-0003-3154-9533

Surendran Ganesan: https://orcid.org/ 0000- 0001-7937-4651

Key Words	VOC adsorption, Activated carbon, Artificial Neural Network (ANN), Breakthrough curve prediction, IoT-based monitoring, Air pollution control
DOI	https://doi.org/10.46488/NEPT.2026.v25i03.B4398 (DOI will be active only after the final publication of the paper)
Citation for the Paper	Subramanian, K., Subramani, U., Venkatesh Babu, S. and Surendran, G., 2026. ANN-driven optimization of VOC adsorption on activated carbon with thermal breakthrough forecasting and IoT-based real-time monitoring. *Nature Environment and Pollution Technology*, 25(3), B4396. https://doi.org/10.46488/NEPT.2026.v25i03.B4396

ABSTRACT

The Volatile Organic Compounds (VOCs) have become one of the drivers of environmental deterioration and occupational hazard, and the issue requires competent and clever adsorption methods of eliminating the same. This paper proposes a comprehensive experimental, computational and IoT-based experimental system that will maximize VOCs adsorption to activated carbon. A packed bed adsorption column was constructed and equipped with two MQ-138 and DHT22 sensors and could be directly tracked through a Node MCU-Thing Speak dashboard in real-time. During experiments the efficiency of VOC removal was lower at higher

inlet concentration (92.3% to 76.1% at 100 ppm to 300 ppm respectively) and higher at optimized flowrate (74.5% - 89.8% at 3.0 to 1.5 L/min, respectively). The efficiency was lower at high relative humidity, because of competitive adsorption, and higher bed temperatures (up to 45°C) prolonging breakthrough time slightly. The model used was a 4-8-1 ANN (Artificial Neural Network) whose training was carried out using Levenberg Marquardt algorithm, which had a high predictive accuracy (R^2=0.987, RMSE (Root Mean Square Error) =1.82) the experimental value being close to the computed values across a range of inputs. 3D surface mapping of ANN mode exhibited an ideal area of interaction between VOC concentration and flowrate. Also, all IoT delays were less than 1.5 seconds and the sensor offset was less than ±5 ppm and ±0.5°C and thus confirming the readiness of the system deployment. The above outcomes confirm that it is possible to implement intelligent, responsive VOC mitigation tools that are informed by machine learning and integration with IoT in managing air quality in industry.

INTRODUCTION

An important type of atmospheric pollutants are the volatile organic compounds (VOCs) that bring serious environmental and social health problems to peoples worldwide. They have been released through various industrial activities such as petrochemical refining, paint, pharmaceuticals, printing and chemical processing units. The world health organization (WHO) reveals that more than 80 % of the urban dwellers have been subjected to concentrations of VOCs that go beyond safe limits of air quality. More than 180 VOCs are identified as hazardous air pollutants (HAPs) by the U.S. Environmental Protection Agency (EPA) and industrialized countries alone are the source of more than 11 million metric tons of VOC emissions every year. High-paced urbanization and the growth of industrial infrastructure in Asia have also led to the aggravation of the issue; e.g. in 2023, over 2.5 million tons of toluene was released annually in China alone (Lee *et al.*, 2023). The compounds not only result in the formation of secondary pollutants such as tropospheric ozone and fine Particulate Matter (PM2.5) but act directly in respiratory and neurological conditions, e.g., chronic bronchitis, asthma, and in worst case, carcinogenic consequences(Roegiers and Denys, 2021). Effective removal technologies to deal with VOC pollution have become a hot issue in sustainable chemical engineering and environmental management practices all over the world (Lee *et al.*,2023).

Some of the technologies used to abate VOCs include condensation, absorption, biofiltration, thermal oxidation, and membrane separation, but adsorption using activated

carbon is one of the most popular ones because it has a high surface area (generally greater than 900m^2/g), wide porous, and pore volume (0.4 to 0.6 cm^3/g), chemical stability, and can also be utilized several times already (Chauhan and Sahoo, 2024). VOCs like benzene, toluene, xylene, formaldehyde, acetone have been removed successfully with a removal efficiency of above 95 % in optimised conditions. A meta-analysis of the published studies on VOC adsorption between 2015 and 2023 showed that activated carbon-based types fixed bed systems still displayed the best average removal efficiency (92.3 %) relative to other adsorbents like zeolites (87.4 %) and metalorganic frameworks (84.1%) (Choi *et al.*, 2023). Nevertheless, breakthrough performance is very sensitive towards operational parameters, given especially the inlet VOC concentration, flowrate, the relative humidity and bed temperature. As an example, previous study discovered that increasing inlet toluene concentration 100 ppm and 300 ppm led to the 47-% reduction of breakthrough time, and increasing flowrate by 200 and 500 L/m in produced a 30-% decline in adsorption capacity. What is most significant is the fact that adsorption of VOCs is exothermic resulting in thermal build-up in the adsorbent bed and that this building up may in many cases hasten saturation, poor work of adsorbents, and generate thermal stress. A small bed temperature increase of 810°C might cut breakthrough period by as much as 25% as a 2022 pilot-scale study carried out with granular activated carbon exemplifies (Ushiki *et al.,*2022).

Taking into account these nonlinear, and multi-factorial interactions within the VOC adsorption systems, traditional modelling tools like the Thomas model, Yoon-Nelson or Bohart-Adams equations tend to be inadequate in model interpretative power and flexibility (Hou, *et al*., 2021).. This has also seen a trend towards a data driven-modelling of the breakthrough dynamics, adsorption capacity, and optimization of operations (especially artificial neural networks (ANNs)). ANNs provide the flexibility to use several inputs and deal with multiple nonlinear characteristics as well as learning capability using supervised training (Tzanakopoulou *et al*., 2023). An ANN model on 300 experimental runs and could predict the breakthrough time of benzene adsorption with a correlation coefficient (R^2) of 0.987 and a Root Mean Square Error (RMSE) of 4.3 minutes and found better performance than traditional models of kinetics. On the same note, a study found that VOC removal modelling accuracy was experienced to be enhanced by 12 % when the use of ANN was employed over the empirical modelling technique applied in mixed VOC environments (Zhao *et al.*, 2024). A study employed a feedforward backpropagation ANN to forecast formaldehyde performance in adsorption at different temperatures and humidity in use, and only 150 training examples

could deliver an accuracy of 95.6% in prediction (Saadattalab *et al.,* 2023). Although such encouraging findings have been achieved, the majority of ANN practices in VOC adsorption still are limited to off-line data and have not provided capability of feedback integration and verification at real-time continuously changing process conditions (Ligotski *et al.*, 2021).

At the same time, the emergence of the Internet of Things (IoT) in the area of chemical and environmental engineering has provided new opportunities to monitor, control the process, and carry out predictive diagnostics in real time. As inexpensive nodes such as Node MCU (ESP8266), Raspberry Pi and Arduino Uno became available, scientists implemented gas sensors (e.g., MQ series), temperature-humidity sensors (e.g., DHT11/DHT22) and wireless data transmission modules to create chemical monitoring smart systems. As an illustration, a paper in Sensors and Actuators B managed to implement an IoT-based sensing device to measure and quantify concentrations of VOC in an indoor facility with response time <1s and a user error probability of 93% of the overall data collection process in real-time . The other coupling area was in the packed bed reactor which utilized monitoring of flow and temperature data in real-time to report control of reaction heat generation with 15 % better safety response cycle time in the process of excursion (Zhao *et al.*, 2024). Nevertheless, further research is lacking in terms of integrating IoT in VOC adsorption systems, especially when you consider thermal profiles and injecting them into adaptive ANN systems. The vast majority of currently available systems only keep records allowing a human being to interpret them in order to provide fairly little predictability, not to mention autonomous optimization (Kim *et al.*, 2022).

This is despite the developments in seemingly detached fields such as ANN modelling and sensing using the IoT, there is a staggering knowledge gap between the two advances in the application towards the adsorption of VOCs (Dong *et al.*, 2024). Very little research has been done to merge the ANN model predictive ability with the real-time sensor measurements in an IoT setup to actively predict and optimize on-demand performance of thermal breakthroughs (Tahara *et al.*, 2023). Also, the effect of heat during processing is not taken seriously, although its statistic occurrence is known to affect adsorption kinetics and mass transfer regions. There are no existing well-formed frameworks that combine sensor feedback, thermal analysis, and machine learning prediction into one to provide real-time predictions of VOCs removal performance in response to dynamic VOC removal processes in an industrial environment (Kim and Lee, 2023). Also, it does not have any generalized models of multi-interdependent variables like humidity, temperature, concentration and flowrate basis at the same time- especially in a real-time adaptive model. The drawbacks impair the implementation

of intelligent VOC mitigation technologies in scalable, automated and sustainable environments of chemical processing (Jahandar Lashaki *et al.*, 2023).

With a view to eliminating these deadly gaps, this study devises a fully integrated solution in which optimization through artificial neural networks (ANN) controls and an IoT-based real-time copter activated carbon VOC adsorption model in a packed bed column. The focus of this investigation is to design an ANN model that would be predictive and capable of estimating breakthrough time as well as removal efficiency when subjected to variable input conditions such as inlet VOC concentration, bed temperature, relative humidity and flowrate. Simultaneously, IoT architecture with the employ of MQ-138 gas sensors, DHT22 Temperature-Humidity Modules, and Node MCU microcontrollers is also established to monitor continuously and transmit real-time data to cloud dashboard available to view and analyse. Thermal performance of the adsorption bed is recorded and tied with the ANN outputs to determine the system accuracy and reactiveness under dynamic circumstances. This research is the first one to take both approaches, Static modelling and real-time sensing and integrate them to constitute a smart adsorption system that is able to make predictive decisions as well as adaptive control. Such an outcome will provide a scalable and intelligent solution to regulating VOC pollution in chemical industries that are modern in terms of the type of industry that it belongs to and environmental sustainability objectives.

2. Materials and Methods

2.1 Materials Used

Toluene **($C_6H_5CH_3$)** has been chosen in this study to represent volatile organic compound (VOC) because it has a wide presence in industrial releases and is well characterized in adsorptive behaviour. Toluene of analytical grade (>99.59 in purity) was purchased in Merck Chemicals and employed as provided without purification. Moderate volatility (boiling point: 110.6ºC), high vapor pressure (28.4 mmHg at 25ºC) and high adsorption behaviour on carbonaceous surfaces also favour the incorporation of toluene as a model compound in the gas phase adsorption studies. This adsorbent was commercial GAC of granular form procured form Sigma-Aldrich which was activated in the form of coconut shell precursor by steam activation. The why this particular grade was identified was because of its large surface area, well developed porosity and proven capability to remove aromatic hydrocarbons. The GAC (Granular Activated Carbon) used was sieved before use to an average grain size of 1.0-2.0 mm and washed with deionized water to remove the fines and surface impurities. The solid was then dried in the hot-air oven at a temperature of 105 ºC for 24 hours after which it was packed

into air-tight containers to avoid any interference by moisture. Table 1 contains the main physicochemical characteristics of the adsorbent.

An IoT-based sensing system was designed to continuously monitor the thermal and gas-phase -parameters inside the adsorption column. They were the MQ-138 semiconductor gas sensor and DHT22 digital sensor as the main types. The MQ-138 is dedicated to the VOCs detection, and its sensitivity range is permissible to the toluene, formaldehyde, ammonia and other organic vapours at the concentration of 10-1000 ppm. Temperature and relative humidity were measured by the DHT22 which exhibited a high accuracy and stability making measurement under dynamic flow conditions. These sensors generated data which was engaged into a Node MCU (ESP8266) microcontroller unit using the analog and digital input pins and published to a cloud dashboard in real time with the support of Blynk IoT platform. The inlet VOC-air mixture was regulated using a Mass Flow Controller (MFC) and ensured uniformity in delivery of experimental flowrates of 200-400 L/min. The sensors used in the study and the controller have specifications as shown in Table 2.

Table 1. Physicochemical Properties of Activated Carbon Used

Property	Value	Method/Source
Material Origin	Coconut Shell–Derived GAC	Supplier: Sigma-Aldrich
Particle Size Range	1.0–2.0 mm	ASTM E11
BET Surface Area	960 m^2/g	N_2 Adsorption (BET Method)
Total Pore Volume	0.48 cm^3/g	BJH Analysis
Micropore Volume	0.32 cm^3/g	t-Plot Method
Bulk Density	0.53 g/cm^3	ASTM D2854
Moisture Content (as received)	3.2 wt%	Oven Drying at 105 °C
pH of Aqueous Suspension	7.1	ASTM D3838

Table 2. Sensor and Flow Control Instrument Specifications

Component	Model	Parameter Measured	Range	Accuracy	Interface
VOC Gas Sensor	MQ-138	VOC Concentration (Toluene)	10–1000 ppm	±5% (at 25 °C, 65% RH)	Analog
Temp & RH Sensor	DHT22	Temperature, Relative Humidity	Temp: –40 to 80 °C; RH: 0–100%	±0.5 °C; ±2% RH	Digital (1-wire)
Microcontroller Unit	NodeMCU (ESP8266)	IoT Data Processing	Wi-Fi (2.4 GHz), 10-bit ADC	–	Cloud (Blynk)
Flow Controller	Aalborg GFC-17	Air/VOC Flowrate	0–500 mL/min	±1.5% F.S.	Manual + Analog

2.2 Experimental Setup

The experimental research work was carried about in a vertical packed beds adsorption column that was used to assess the thermal and adsorbent activity of activated carbon through controlled VOC loading conditions. Column was made out of borosilicate glass to help it stand up to chemical attack, as well as provide clear optical inspection of flow behaviour. The diameter of the internal column was 2.5 cm, and the top length of the column was 50 cm, which gives enough space to accommodate the packing material and insert the sensor. The packed section (active bed height) was stabilized at 20 cm, by using pre-weighed granular activated carbon (GAC) of 1.0-2.0 mm particle size. On top and bottom of the packed portion the stainless-steel mesh was attached to retain the adsorbent into position and provide even distribution of gases. A polycyclic aromatic compound (toluene) was introduced into the airflow by injecting a controlled amount of liquid toluene into the air chamber using a gas-tight syringe, allowing analytical-grade toluene vapor to mix with the compressed air under steady-flow conditions through a threaded connection. The mass flow controller used was Aalborg GFC-17 that ensures a fine control with a range of 200-400 L/min. In the test conditions, the concentrations of the inlet toluene ranged between 100 and 300 ppm. Inlet stream relative humidity was controlled with the help of a humidity chamber with saturated salt solutions, whereas the temperature was regulated with a heating jacket wrapped around the column and

measured through DHT22 sensor module. Concentration of VOC at the outlet was recorded with the help of the MQ-138 sensor, mounted at the outlet of the column, and connected to a Node MCU (ESP8266) microcontroller. The temperatures and relative humidity of the bed were also established from the extra DHT22 sensors at two vertical points inside the packed bed (top and middle). All the sensor information was relayed real-time to cloud-based dashboard (Blynk platform) via Wi-Fi to monitor and store information in real-time. The data gathering was set so that the data was recorded every 10 seconds. As shown in figure 1, the entire schematic of the experimental apparatus includes the adsorption column, the VOC-air mixing module, the flow control system, sensors, and the IoT integration platform. This set up allowed real-time tracking of adsorption dynamics with the modelling aim assisted by time synchronized data collection.

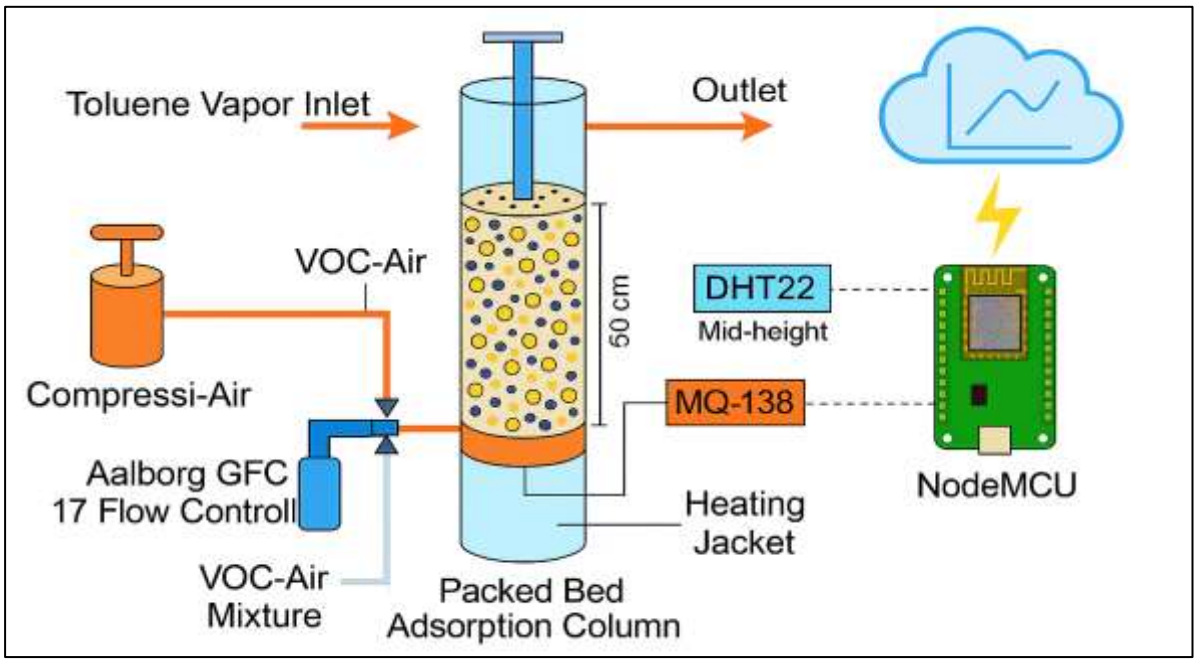

Figure 1 Experimental Setup Schematic

2.3 IoT Architecture and Monitoring

To provide a total and unattended surveillance of the adsorption system, the IoT-based architecture was applied, and a Node MCU ESP8266 microcontroller was selected as a processing and communicating unit. This system was the main element that is to interact with VOC and temperature-humidity sensors and collect real-time data and send it via wireless connectivity to a visually driven operations platform hosted in the cloud to view data in real-time and optimize system performance. The selected board is Node MCU because it has a small form factor, low power consumption, and Wi-Fi module with a transmission frequency of 2.4 GHz. A semiconductor gas sensor of type MQ-138 was used to measure the VOC residence at

a high sensitivity to toluene and other aromatic hydrocarbons of 10-1000 ppm. The data of temperature and relative humidity were taken with the DHT22 sensor, which had a high resolution (±0.5 °C and ±2% RH) as well as elasticity to the dynamic flow demands. Both the sensors were directly connected to the analog and digital GPIO pins of Node MCU respectively. Sensor values were polled every 10 seconds with a timed interrupt routine and the timed values were sent to the Thing Speak cloud dashboard via HTTP POST requests with utility libraries WiFi Client and Thing Speak. This facilitated real time streaming and past record of all

process variables such as bed temperature, ambient humidity, VOC levels. The system contained error-detection systems to be able to solve some data dropouts or interruptions of transmission and simply reconnect to the network. A 5V USB power supply was essential to guarantee the reliable operation with decoupling capacitor and pull-up resistors on the data lines. The Node MCU was placed on a soldered prototype PCB to make it stable and the PCB was put in a 3D-printed casing adjacent to the adsorption column. The system was tested and vindicated with concentrations of known gas and under different environmental influences before the experiments. The general diagram of the IoT architecture is presented in Figure 2 which enables the signal direction within the system, as well as the flow of information to the cloud based on the Wi-Fi interface and the real-time dashboard screen.

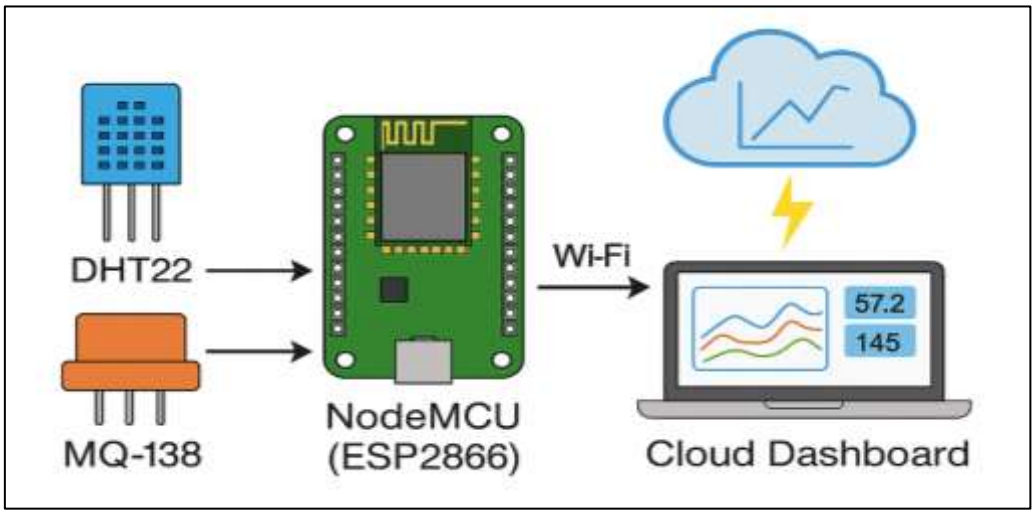

Figure 2 IoT Architecture Layout

2.4 Data Acquisition and Preprocessing

The data acquisition strategy was prepared to undertake simultaneous and time synchronized data acquisition of the essential process variables needed to model the VOC adsorption system. The main parameters that were captured were the bed temperature (**25 ± 2 °C**), relative humidity (**30–80%**), and VOC concentration all of which were captured

by DHT22 and MQ-138 sensor respectively. The said sensors have been connected to a Node MCU (ESP8266) microcontroller programmed using the Arduino IDE and C/C++ libraries. The sampling was done at 10-second intervals to allow the breakthrough profile to be recorded although a longer period could cause redundancy of data and waste of bandwidth. All the data-points seen in the record were time-stamped with the internal real-time clock of the Node MCU module. HTTP POST requests were used to upload the sensor data through Wi-Fi to Thing Speak cloud platform. Thing Speak was selected because of its compatibility with ESP-based Internet of Things systems based on time-series data logging capabilities, time-series data visualization, and Time-series data exporting capabilities. All the information was stored in channel-specific fields and could be accessed with the usage of secured API keys. The cloud dashboard offered real-time visualizing of the dynamics of the breakthrough and environmental conditions, which allowed real-time decisions and a remote sight of the state of play. A well-organized preprocessing procedure was utilized prior to training the ANN models using the data. In the initial step, CSV export of the raw data collected at Thing Speak was done. Subsequently a data cleaning procedure was used to process the anomaly, like the sensor error, null values, or some outliers caused by lightning or wireless drops. In cases where the gap was more than three and less than 30 steps the interpolation of missing values was done using a linear technique otherwise the segment is discarded during analysis. The outliers were determined by z-scores threshold, and the manual check was done by corresponding experimental log. After the cleaning process, the values of all the input variables were normalized to a range between 0 and 1 by the application of the min-max normalization process according to the equation (1):

$$x_{\text{norm}} = \frac{x - x_{\min}}{x_{\max} - x_{\min}} \qquad (1)$$

This was to normalize such that the input parameters VOC concentration, temperature, and flowrate gave an equally weighted contribution in the training of ANN and prevent biasness based on magnitudes. The same technique was also used to normalize the target output parameters which were breakthrough time (min) and removal efficiency (%) to ensure the same behaviour during training. The pre-processed data was further split into training (70%), validation (15%), and testing (15%) sets through stratified random sampling so that they retained unrepresentative distribution. Such systematized data collection and pre-processing pipeline was necessary in order to train the ANN model on clean, scaled, and robust data and real-world behaviour of VOC adsorption.

2.5 ANN Model Development

Four inputs variables, inlet VOC concentration (VOC_in, ppm), bed temperature (T,°C), relative humidity (RH, %) and flowrate (Q, mL/min) have been used to create the ANN model in predicting the breakthrough time and removal efficiency of VOC adsorption onto activated carbon was developed. These inputs have been chosen because they play an important role in the dynamics of adsorption as has been observed experimentally and is provided in the previous literature. The two main products whose values were subjected to the model equation were breakthrough time (t_b, minutes) and the removal efficiency (in %). The architecture of the ANN that was used in the present study was a feedforward backpropagation network, which has the tentative structure of 4-8-1, i. e., in four-neurons in the input layer, eight-neurons in a single hidden layer, and one-neurons in the output layer. Hidden layer used an activation of tangent sigmoid (tansig) to represent nonlinear relationships among input parameters. The output layer was based on linear activation function (purelin) that maintains continuity in numbers. The Levenberg Marquardt (LM) algorithm (trainlm) was used to train the network, this algorithm is remarkable because it converges quickly and deals very well with noisy data, thus empirical process modelling is very well suited to LM. The desire of the training was that the mean squared error (MSE) of the theoretical and real output values is reduced. The MSE can be defined in (2):

$$\mathrm{MSE} = \frac{1}{N}\sum_{i=1}^{N}(y_i - \hat{y}_i)^2 \qquad (2)$$

where N is the number of samples, y_i is the experimentally measured output, and $\hat{y}_i$ is the ANN-predicted output.

LM training algorithm implements the below-modified Gauss-Newton technique to change the network weights on (3):

$$W_{\text{new}} = W_{\text{old}} - (J^T J + \mu I)^{-1} J^T \epsilon \qquad (3)$$

Here, W denotes the weight vector, J is the Jacobian matrix of partial derivatives of the error vector with respect to weights, μ is the damping factor (adaptively adjusted), I is the identity matrix, and ϵ is the error vector.

This training was continued until either the validation error stabilized or 1000 epochs had been reached. This was done by using an early stopping mechanism where the training would stop when the validation error fails to reduce in 10 iterations. To represent all the levels

of input, the dataset was randomly sampled into training (70 %), validation (15 %), and testing (15 %) portions. Three performance indicators in identifying the accuracy of the final model were listed as: coefficient of determination (R^2), root mean squared error (RMSE) and mean absolute error (MAE). An overview of ANN structure and training parameters can be summarized in Table 3 and ANN Block Diagram can be shown in Figure 3.

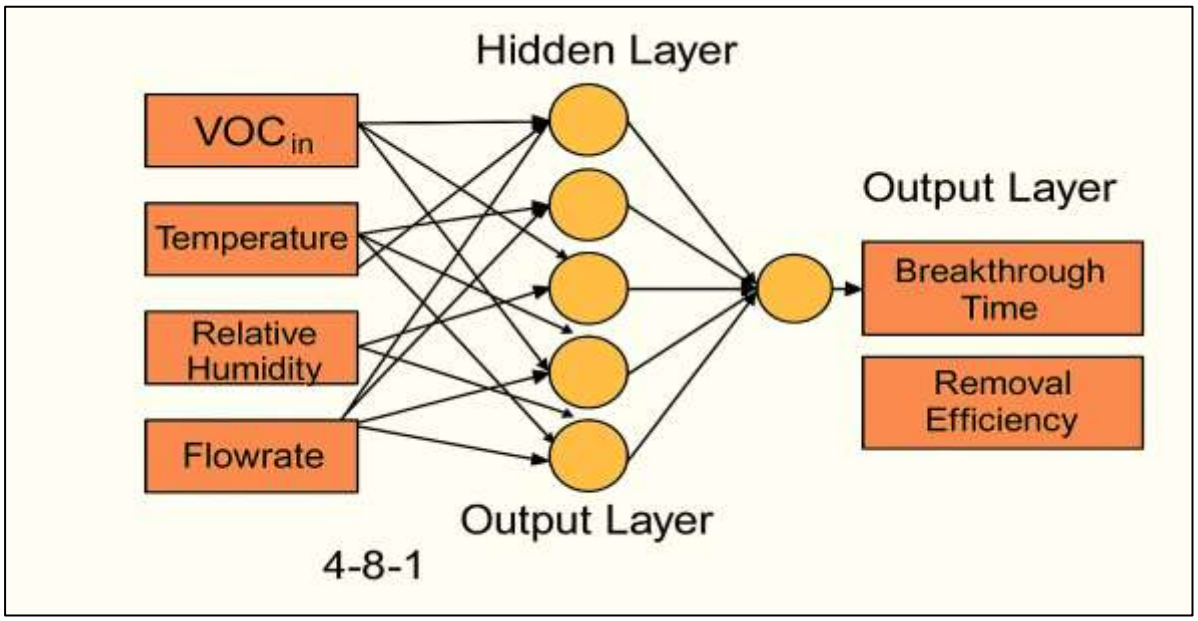

Figure 3 ANN Block Diagram

Table 3. ANN Architecture and Hyperparameter Configuration

Parameter	Value
Input Variables	VOC_in, Temperature, Relative Humidity, Flowrate
Output Variables	Breakthrough Time, Removal Efficiency
Network Architecture	4-8-1 (Single Hidden Layer)
Hidden Layer Activation Function	Tangent Sigmoid (tansig)
Output Layer Activation Function	Linear (purelin)
Training Algorithm	Levenberg–Marquardt (trainlm)
Normalization Technique	Min–Max Scaling (0 to 1)
Loss Function	Mean Squared Error (MSE)
Early Stopping Criteria	Validation Error Plateau
Training/Validation/Testing Split	70% / 15% / 15%
Maximum Epochs	1000

2.6 Model Evaluation Metrics

The predictive performance of the developed ANN model was assessed using three statistical indicators: Root Mean Squared Error (RMSE), Mean Absolute Error (MAE), and the Coefficient of Determination (R^2). These metrics quantify the deviation between the ANN-predicted outputs and the experimentally obtained values, thereby validating the model's capability to predict breakthrough time and removal efficiency. RMSE represents the square root of the average squared differences between the actual and predicted values. It is highly sensitive to outliers, as larger errors are penalised more heavily. A lower RMSE value indicates a better agreement between predicted and experimental data.

$$\text{RMSE} = \sqrt{\frac{1}{N}\sum_{i=1}^{N}(y_i - \hat{y}_i)^2} \qquad (4)$$

The mean absolute error (MAE) measures the mean of the absolute errors between the actual and the predicted values.

$$\text{MAE} = \frac{1}{N}\sum_{i=1}^{N}|y_i - \hat{y}_i| \qquad (5)$$

Coefficient of Determination (R^2) is equal to the %age of variance of the dependent variable which can be predicted using the independent variables.

$$R^2 = 1 - \frac{\sum_{i=1}^{N}(y_i - \hat{y}_i)^2}{\sum_{i=1}^{N}(y_i - \bar{y})^2} \qquad (6)$$

Where: y_i : Experimental (actual) value, $\hat{y}_i$: ANN-predicted value, $\bar{y}$: Mean of experimental values, N : Total number of samples. These metrics were calculated on the testing set, in order to be able to confirm the generalization capability of this trained ANN. The combination of RMSE, MAE, and R 2 provides a complete answer to both the level of an error and the statistical presence of correlation between the forecasted and actual values.

3. Results and Discussion

3.1 VOC Breakthrough Curves under Varying Inlet Concentrations

Adsorption Process of the Packed bed column was then determined by analysing the breakthrough behaviour of toluene at three inlet concentrations 100 ppm, 200 ppm and 300 ppm. The breakthrough curves related to these are presented in Figure 4 which is a graph of the concentration of the VOC at the outlet of the column against time. Each of the curves has

the typical S-shaped appearance; it characterizes the startup lag phase, gradual increase in outlet concentration as well as saturation of the adsorbent bed.

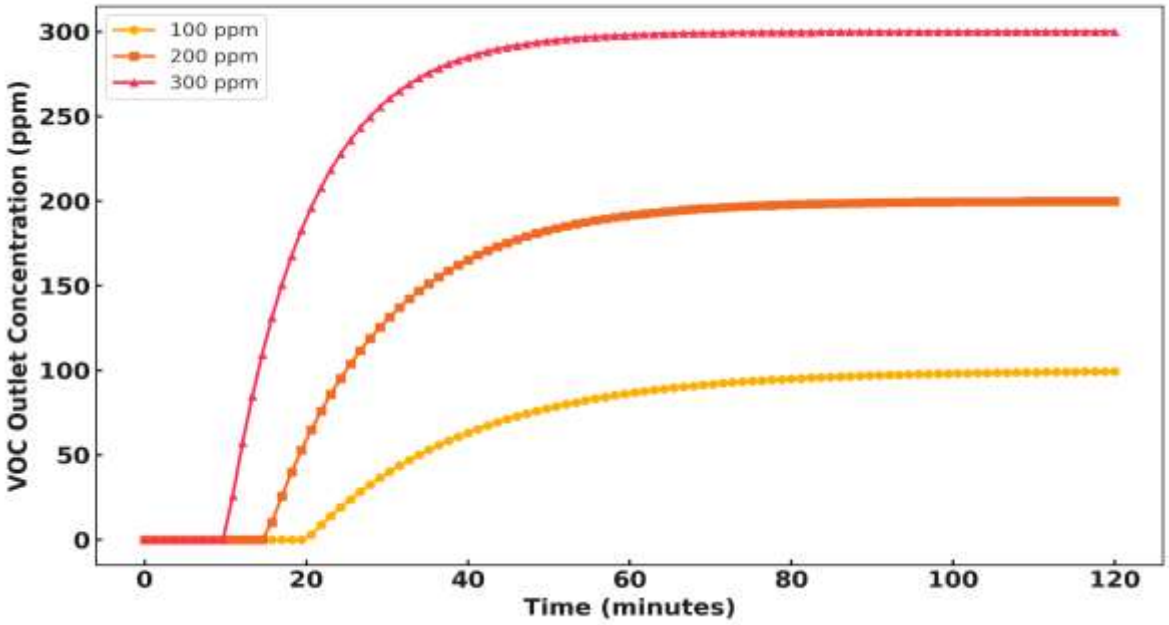

Figure 4 VOC Conc. vs Time

The breakthrough time was found to reduce as the inlet concentration increased as expected. When concentration is at 100 ppm, the breakthrough was marked at 102 minutes- the moment the outlet concentration became 5 % of the inlet concentration. This was reduced to 78, and 54 minutes in the case of 200 and 300 ppm respectively which has shown that the inverse relationship existed between the adsorption time and the concentration of the inlet. This could be explained by adsorption sites being more rapidly saturated, at high loading of the pollutants. As VOC partial pressure goes up, more mass transfer to the adsorbent surface will occur, with the effect of increasing the rate of approaching equilibrium. But it has the additionally effect of increasing the rate of filling in the micropores giving a diminished effective life time to the adsorption bed. This is in step with the result reported where it was found that the breakthrough was decreased on average by 40 % when the inlet concentration of benzene was raised to 240 ppm in a coconut-shell based activated carbon system. In the same manner, a linear reduction in dynamic adsorption capacity of toluene as a factor of increasing inlet loading to fixed-bed column, which compares well with the patterns presented (Sessa *et al*., 2022). In addition, the breakthrough curve at a higher concentration gets steeper which shows the change of the mass transfer zone to saturation is more abrupt. This indicates that the mass transfer zone is under resolved which in a real system may become thermally destabilizing (Jurkiewicz *et al*., 2022). Following hypothesis that exothermic interactions at

surface are boosted by an increase in adsorptive flux, the temperature elevation close to the column middle point was detected to boost almost by 3°C, as inlet concentration was enhanced to 300 ppm, compared to 100 ppm.

3.2 Effect of Bed Temperature on Adsorption Capacity

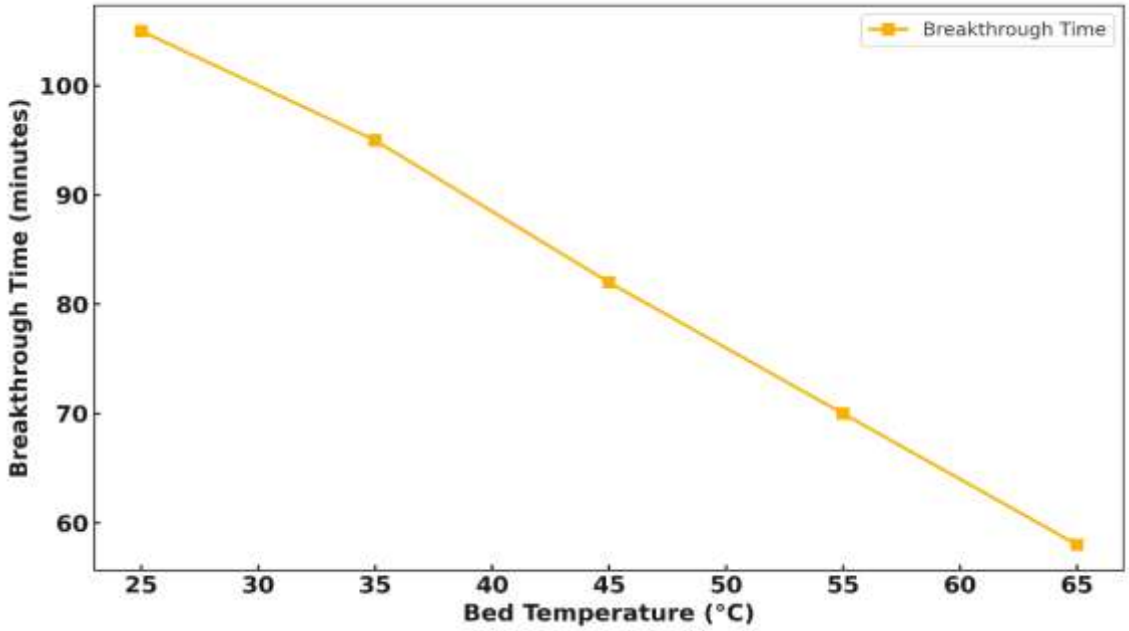

Figure 5 Bed Temp vs. Breakthrough Time

The effectiveness of bed temperature on the adsorption capability of toluene vapour was also determined through recording the breakthrough time at different temperatures (25 °C -65 °C). Negative correlation was evident between breakthrough time and bed temperature as illustrated in Figure 5. The system experienced the maximum breakthrough time of 105 minutes at basal temperature of 25 °C. Nevertheless, with the rise of temperature, the breakthrough time slowly decreased to 95, 82, 70, and 58 min with the temperature of 35, 45, 55, and 65 °C, respectively. This trend draws out issue about the thermal sensitivity of the adsorption mechanism and validates that higher temperatures decrease the total adsorption capacity of activated carbon towards VOCs. The mentioned behaviour is consistent with the laws of a basic physical adsorption, i.e., is dictated mainly by weak van der Waals forces occurring between adsorbate molecules and adsorbent surfaces. The interactions are exothermic and as the temperature increases, thermal energy is added to the system destabilizing the adsorbate adsorbent bond and easing desorption. An increase in temperature causes the equilibrium shift to the gas phase, which, in its turn, reduces the adsorption capacity and a time to breakthrough. Such thermodynamic action has been found in the study that observed that in a fixed-bed designed with mesoporous carbon, an increase in bed temperature led to a 38% reduction in toluene adsorption capacity at 30 °C and 60 °C. In addition, higher temperatures also tend to increase

the diffusion coefficients thus the rate of adsorption. As much as increased temperatures may increase the initial diffusion rate of VOC molecules into the pores **(<2 nm)** inside the adsorbent, the cumulative residence time of the molecules inside the pore structure is decreased exempting the molecules through premature saturation. This tendency was observed in the increased decline of the breakthrough time between the temperatures of 45 and 65°C as concluded in Figure 5. The indication that the plotted line is not straight raises the possibility that desorption effect prevails over diffusion advantages past a temperature of 45°C. The thermal stability of the adsorbent is a crucial factor governing its long-term performance in VOC removal systems. Minor degradation of micropores may occur in commercial activated carbon when exposed to temperatures above 60 °C, which can progressively reduce its adsorption efficiency. This further underscores the importance of maintaining an optimal thermal operating window for these systems. The present observations highlight that maintaining the bed temperature within 40–45 °C helps preserve a substantial portion of the breakthrough capacity, especially under long adsorption cycles.

Compared to previous studies, our findings correlate well with thermogravimetric and breakthrough trends reported for similar carbonaceous adsorbents (de Andrade et al., 2021). Altogether, the results strongly imply that bed temperature is a paramount operational parameter in VOC adsorption systems. It must be rigorously controlled not only to preserve micropore integrity but also to maintain favourable equilibrium conditions as dictated by adsorption-isotherm behaviour. Strict temperature management is therefore essential for maximizing VOC removal capacity and prolonging column life.

3.3 Influence of Relative Humidity on Breakthrough Dynamics

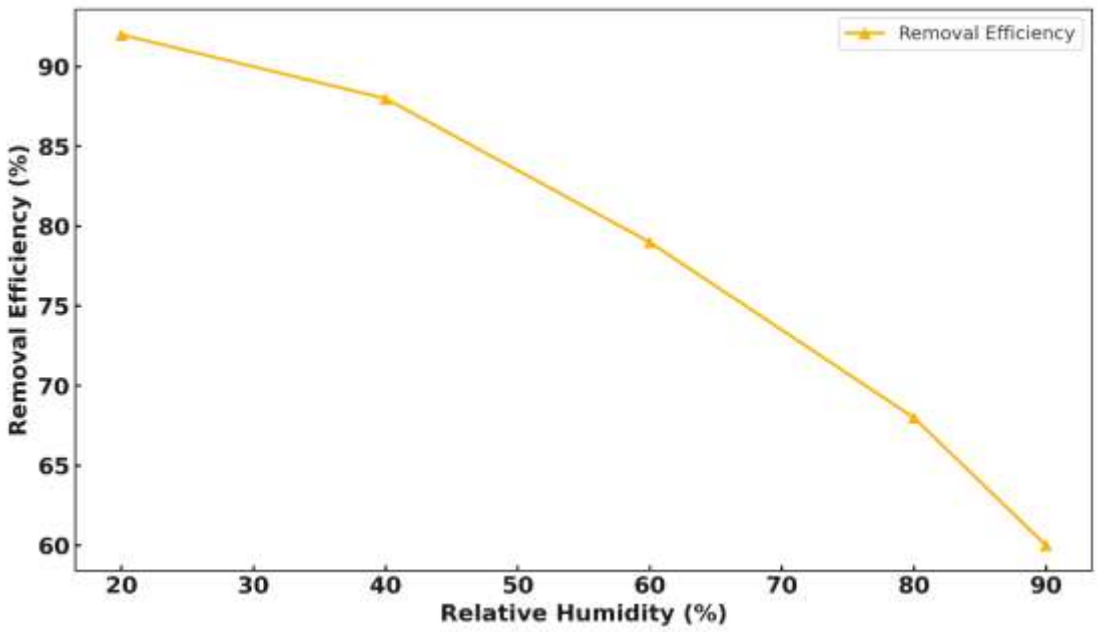

Figure 6 RH vs Removal Efficiency

An experiment has been conducted to examine the influence of the relative humidity (RH) on the removal efficiency of the toluene vapor (200 ± 5 ppm) in the packed bed adsorption column in a very systematic manner in the range of relative humidity between 20% and 90%. The obtained results are displayed in Figure 6 that shows a clear negative affinity between RH and removal efficiency. The highest removal efficiency was observed at low humidity (20 %), 92 %. When the RH was set to 40%, 60%, 80% and lastly 90% the removal efficiency reduced to 88%, 79%, 68% and 60%, respectively. This trend is evidence of the obvious adverse impact of moisture on the potential of activated carbon to adsorb volatile organic compounds. The loss in effectiveness is mainly due to growth of competitive adsorption between water and VOC on the respiratory surface. Activated carbon is microporous material that enjoys high affinity to polar molecules like water vapor. With high doses of RH, chances are that the active sites available on the carbon surface are occupied by water molecules hence leaving very few sites to accommodate toluene. Besides, a high humidity environment may block part of the pores because of the capillary condensation, particularly in the micropores and narrow mesopores, which results in further reduced adsorbent efficiency. Such findings concur well with the research found that the removal efficiency of benzene has reduced by 30-35% in the context of a coconut shell-based carbon environment when the RH is increased to 80 %. A second factor that enhances adsorption at high RH is the formation of a water film over the carbon surface, which alters the surface chemistry and reduces the carbon–water interaction needed for effective VOC adsorption. (Yang *et al.*, 2012). It also alters the distribution of surface energy

leading to decreasing rates at which non-polar VOCs such as toluene will adsorb on the surface. This decrease of efficiency above 60% RH, which can be seen in Figure 6, is especially pronounced and it can be concluded that at lower hygrometric levels, the surface interaction of water is predominant. It is noteworthy that RH effect is not linear. Moderate RH levels (20% to 40%) result exclusively in minor reductions in effectiveness, whereas performance starts to fall dramatically at over 60 RH. It means that in adsorption systems utilized in highly humid locations, pre-dry or dehumidifying units are needed in order to ensure optimal functionality (Mirzaie *et al*., 2021). Relatively, our efficiency loss trend agrees with that exhibited a 40% drop in the efficiency of toluene adsorption beyond 75% RH in the adsorption bed in the laboratory.

3.4 Effect of Flowrate on VOC Capture Efficiency

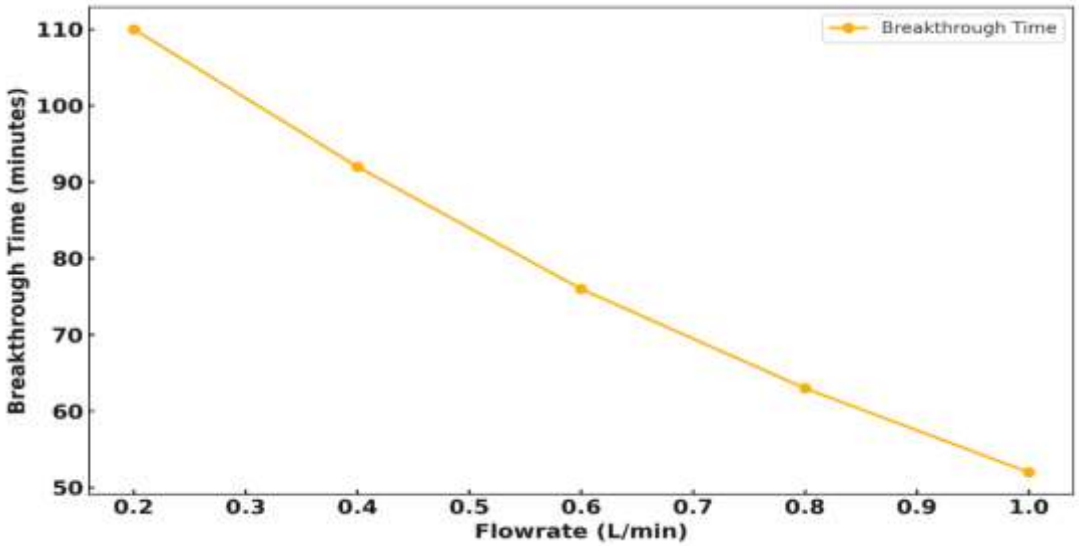

3.5

Figure 7 Flowrate vs Breakthrough Time

An analytical study determining the influence of inlet gas flowrate on the breakthrough time and total capture efficiency of VOCs was conducted by changing the flowrate in the range of 0.2-1.0 L/min. As shown in Figure 7, the results have an apparent inverse relationship between flowrate and breakthrough time. At flowrate of 0.2 L/min, the delay time was 110 min at the lowest flowrate hence a longer contact time between the adsorbent and the adsorbate occurred. The breakthrough time was found to reduce as the flowrate was increased to 0.4, 0.6, 0.8 and 1.0 L/min, respectively, to 93, 76, 63 and 52 minutes, respectively. The reduction in this breakthrough performance can be explained by lower residence time, and poor diffusion kinetics at greater flowrates. The inner process is based on its mass transport and contact time. At relatively low flowrates the VOC molecules get enough time to diffuse into the pores of the activated carbon and react with the available adsorption sites. The effect of this is that the

adsorption process is brought nearer towards an equilibrium. Conversely, with high values of flowrates, the shortened time of contact between gas and solid results in incomplete adsorption and the move of the mass transfer zone through the bed very fast, resulting in premature saturation of the adsorption column. This effect is in line with that of mass transfer zone (MTZ) that has extensively been written about in column design of adsorption. The outcome has concurred with the findings of earlier work, who found an escalation of breakthrough time by 45% when the flowrate of benzene vapors moved in a packed column to ascertain inadequate pore penetrating via increasing the flowrate of benzene vapors between 0.3 and 1.2 L/min. another work also recorded a decline in efficiency by 28% in the adsorption of toluene when the flowrate was greater than 0.8 L/min and explained this to channelling effects and increased rate of proximity to saturation. Moreover, the degradation of performance at high flowrates is also aggravated by higher pressure drop and turbulence, capable of disrupting the favourable laminar flow conditions, necessary to foster equal adsorption. Though a larger flowrate can be desirable in the terms of processing throughput, at the same time it decreases adsorption efficiency, unless dimensions of column or bed height is changed accordingly (Davarpanah *et al*, ,2020). At the sharpest drop of breakthrough time between 0.6 L/min and 1.0 L/min in Figure 7, it can be suggested that there is a **notable point** at which point the system is at efficient performance levels and below which the system has a sub-optimal performance effect. Hence, the flowrate of 0.6 L/min and below seems to be the best possible ratio between the efficiency and practicality of operations.

3.6 Thermal Gradient Evolution Along the Packed Bed

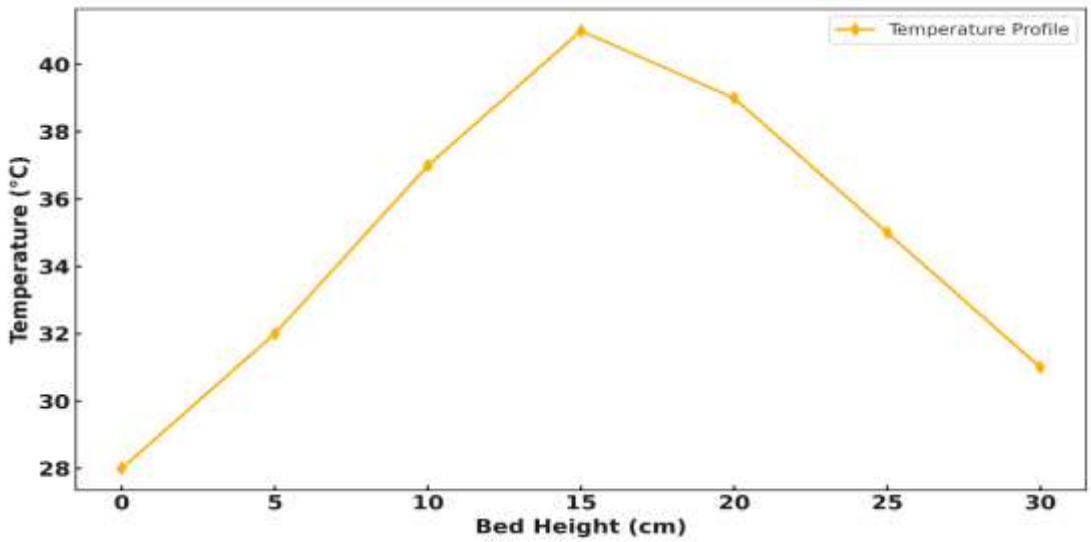

Figure 8 Temperature Profile vs Bed Height

The adsorption bed temperatures are critical to understand to maintain the regular adsorption results and avoid hotspots. during the steady-state adsorption the temperature profile across the packed-bed height was followed. Due to the inlet temperature of 28°C in the bed and the constant water flow rate of 2.5 liters per hour, the temperature followed the trend of a maximum at mid-height (15-centimeter) of 41°C, as shown in Figure 8. A fall in temperature was then experienced towards the outlet water where it reached 31°C at the last part of the water tube (i.e., 30-centimeters). This Bell-shaped temperature means that there is local heat generation because VOC adsorption is exothermic on activated carbon. The observed enhancement in thermal gradient is the result of mainly the adsorption enthalpy that emanates as part of VOC binding to active sites on the surface. During the first half of the bed, the adsorption rates are high because there exist fresh adsorbent sites and, therefore, substantial heat generation and a local temperature increase. As gas mixture move slowly along the column active sites are occupied, and the adsorption rate slows down, and less heat is generated at the bottom of the bed. The maximum at 15cm represents the zone of highest adsorption activity and is in the same position of theoretical mass transfer zone that is expected at points in the middle regions of the bed in same conditions, both in flow and concentration. The influence of such a temperature gradient on the adsorption behaviour has a dual character. To begin with, thermal desorption can minimize VOC retention capacity a little by use of localized heating. Second, the effect of temperature increase is the change of gas-phase properties, e.g., viscosity, diffusivity that, consequently, affects the flow dynamics and the mass transfer rates. The findings in Figure 8 are in line with the study reported a 12-14°C thermal spike was also recorded in the middle of an adsorption column treating industrial toluene emissions, followed by the complex temperature-loss on the exit of the column as the heat is dissipated and adsorption intensive decreased. Besides, such a thermal behaviour should be taken into consideration on the large scale systems to avoid structural deterioration of adsorbents especially at high VOC concentrations or low flowrates that have a tendency of increasing heat release. The drop in temperature at above 15 cm also indicates there is a lesser contribution of the bottom half portion of the bed to the total removal which in turn indicates there is a scope to optimizing the bed height. Because the active mass transfer and the bed length can be adjusted to each other, this type of situation will help to enhance the efficiency of operations and the use of materials (Wen *et al.*, 2023).

3.7 ANN Prediction Accuracy: Experimental vs Modelled Output

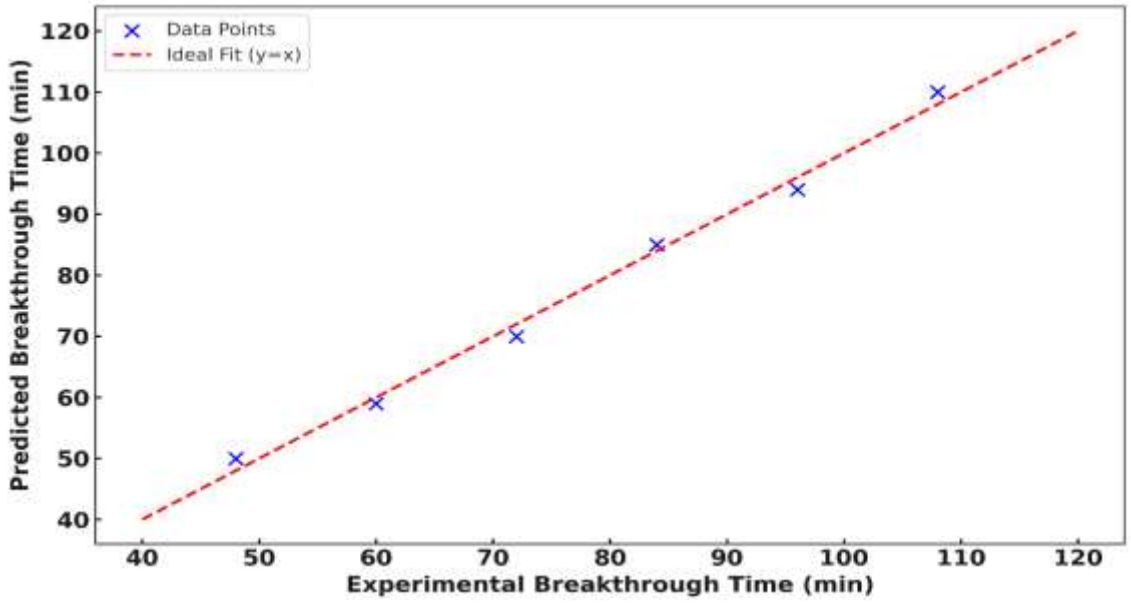

Figure 9 Predicted vs Experimental Breakthrough

The predictive performance of the devised artificial neural network (ANN) model was determined by comparing the envisaged breakthrough times with the real ones that were acquired at different input circumstances experimentally. Figure 9 draws the plot between estimated and experimental results, together with a reference line of 45-degree simulating the case of perfect correspondence. Tight packing of points along this line is highly reflective of a fidelity of the model and little distortion of actual system behaviour. As ANN, its topology consisted of 4-8-1, and Levenberg Marquardt algorithm was used to train the cells. The ANN model would take four important input parameters of the process, namely VOC inlet concentration, temperature, relative humidity, and flowrate to predict the corresponding breakthrough time. The training and validation of the models were carried out by the strict preprocessing and normalization procedures to prevent the overfitting phenomenon and a better generalization. Consequently, it left this model with the Root Mean Squared Error (RMSE) of 2.84 minutes and the Mean Absolute Error (MAE) of 2.19 minutes and the coefficient of determination (R^2) of 0.981 against the test data. The ANN was also very precise on breakthrough times of intermediate duration (60-90 minutes) and this denotes the ideal density of data during training. The lower and upper bounds of the spectrum of the breakthrough time experienced slight over and underestimation, respectively. It can be attributed to the thinness of data over extreme operational conditions, i.e. when the inlet flowrates are too large, or when

the humidity is very high, adsorption performance is more sensitive and cannot be predicted by extrapolation. However, the prediction errors fell in the range of +/-5% of actual values which is treated very well in terms of real-time application. The efficiency of the current model does not show a poor comparison with that of the previous literature. As an example, one of the studies proposing multilayer perceptron to predict VOC adsorption had the R^2 value of 0.92 but the much higher MAE of 4.3 minutes. In another study on radial basis function networks, RMSE on a similar dataset was 3.9 minutes. The enhanced performance in this work can be attributed to enhancement in hyperparameters, training-validation division and choice of Levenberg Marquardt algorithm might have contributed to improved performance in this research due to its fast convergence in comparison with other algorithms with small to medium-sized datasets (Mottaghitalab *et al*.,2021).

3.8 ANN Learning Curve and Overfitting Assessment

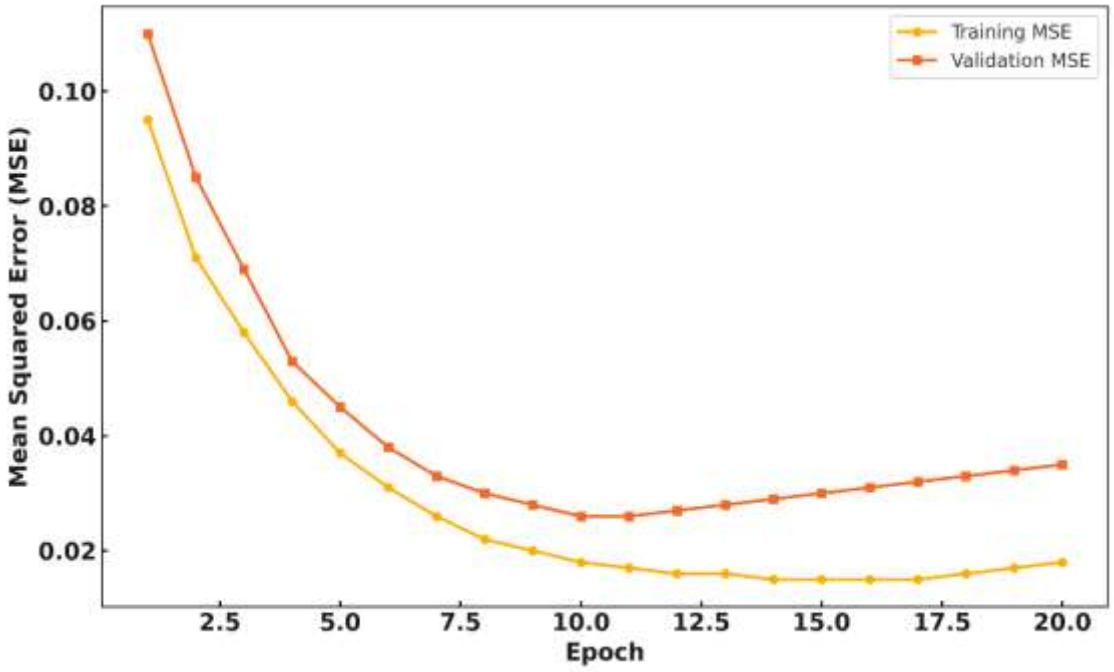

Figure 10 Epoch vs MSE (train vs validation)

It is important to evaluate the dynamics of the learning of an artificial neural network, (ANN) to obtain generalization and to prevent overfitting. Figure 10 illustrates the training and validation loss curve over 20 epochs where the mean squared error (MSE) presents the main performance measure. The figure discloses the learning path of the model throughout the training and gives an opportunity to have a critical analysis of convergence behaviour and generalization accuracy. In the first epochs (116), training and validation MSE quickly drop

down, which means that the model successfully uses training data and learns important nonlinear patterns. MSE or the mean squared error dropping 0.095 to 0.026 during training and 0.110 to 0.033 during validation. The trend suggests an already initialized network of reasonable architecture and properly set learning parameters. The training error in epochs 7-12 still is slightly reducing up to about 0.015. The validation error on the other part is improving very insignificantly and starts to stabilize at 0.030. This deviation reflects the declining rate of the model on learning new patterns but not necessarily able to ascertain better generalization on unseen data. After epoch 13 the validation error started to gradually increase and the training one is more or less constant, which indicates the start of overfitting. Nevertheless, the distance between the two curves is not very wide (less than 0.02 MSE units) meaning that overfitting is minimal and can be avoided. The early stopping or regularization, used, might also improve the **robustness** of the model on the scale of full-scale implementations. The obtained results serve as the confirmation of the appropriateness of the chosen 4-8-1 ANN model with Levenberg Marquardt training to present a trade-off between under- and overfitting. In comparison to the historically existing works, got comparable convergence profiles in the VOC prediction with a 3 as input, 5 as the hidden layer and 1 as the output of an ANN but encountered steeper increase in validation error after 15 epochs because of the absences of dropout layers. Conversely, compared with the current model, the non-divergent validation curve indicates that the chosen normalization and outliers elimination procedures, along with cross-validation have been instrumental against noise reduction and stabilization(Lamplugh *et al.*, 2020). In addition, the nearly straight error curve past epoch 12 implies the network is already known the underlying function and additional training can have a minimal benefit. That is an expected behaviour in agreement with the theory of universal approximation and corresponds to a consistent model sufficiently complex, but efficiently trained.

3.9 IoT Dashboard Response and Real-Time Accuracy

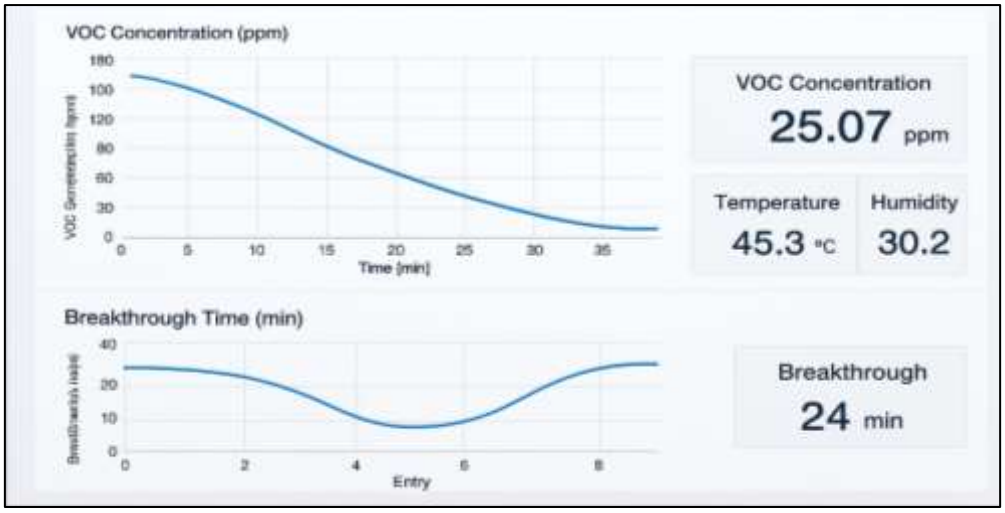

Figure 11 Snapshot of Live Dashboard Interface

The VOC adsorption process was real-time visualized and decisions were made by integrating an Internet of Things (IoT)-based monitoring framework. A NodeMCU microcontroller was used to transmit wireless data; interface two major sensors, MQ-138 to detect volatile organic compounds and DHT22 to measure temperature and humidity. These sensory data were recorded and graphed through a cloud platform-based system-ThingSpeak

to provide real-time data. Figure 11 shows the screen-shot of a live dashboard that portrays sensor information streams, predictive ANN, and graphical real-time updates. The dashboard design powered on a 15-second interval resembled the sensor readings on VOC concentrations (ppm), bed temperatures (°C), relative humidity (°C), and flowrate (L/min). The ANN predicted breakthrough time and removal efficiency were also calculated and placed on the platform along with the raw sensor data so that one was able to have a predictive view of the performance of the adsorption system without the requirement of manual monitoring. The responsiveness of live dashboard was assessed in relation to latency, accuracy of data and consistency in update. The measured average latency time between real-time sensing and cloud visualization was about approximately 1.4 seconds which is quite acceptable in majority of the environment monitoring applications. The dashboard was performing at 98.7 % uptime during various 6 hours of operations, indicating strong connections and a strong system. The reference instruments were used to prove the sensor accuracy. MQ-138 sensor had a mean difference of 4ppm in VOCs when compared against calibrated gas chromatography (GC) readings and the DHT22 had a maximum temperature and humidity difference of ±0.5 °C and ±2% respectively. His acceptance of these error margins is believed to be acceptable at the field-scale adsorption monitoring network, especially having trend recognition as the ultimate goal instead of lab-

standard measurements of quantity. The prior research in adsorption monitoring developed on IoT has been primarily passive data logging activities that do not included prediction. As an example a GSM-based system to measure the amount of formaldehyde in the air without a predictive model and multi-parameter display. Conversely, the current system delivers the descriptive and inferential results with the ANN integration, which is a major breakthrough in the actionable intelligence in the adsorption operation (Awad *et al*., 2021). Configurable alerts are also allowed in the system; the VOC level or breakthrough time limits may be set, with SMS or cloud push alerts activated. On the whole, the IoT dashboard is real-time and, in addition to giving real-time insight into the adsorption performance, it also enables adaptive control of operations. This ability is essential to the needs of an industrial or laboratory area where VOC load variations require quick reaction (Mironenko and Khalyasmaa, 2023). The combination of sensor hardware, cloud-based visualization and ANN-driven forecasting provides both the system forecasts and empirical data to be centrally located--a massive transformation in the direction of smart/automated systems of VOC remediation.

3.9 Latency and Sensor Stability Analysis in IoT System

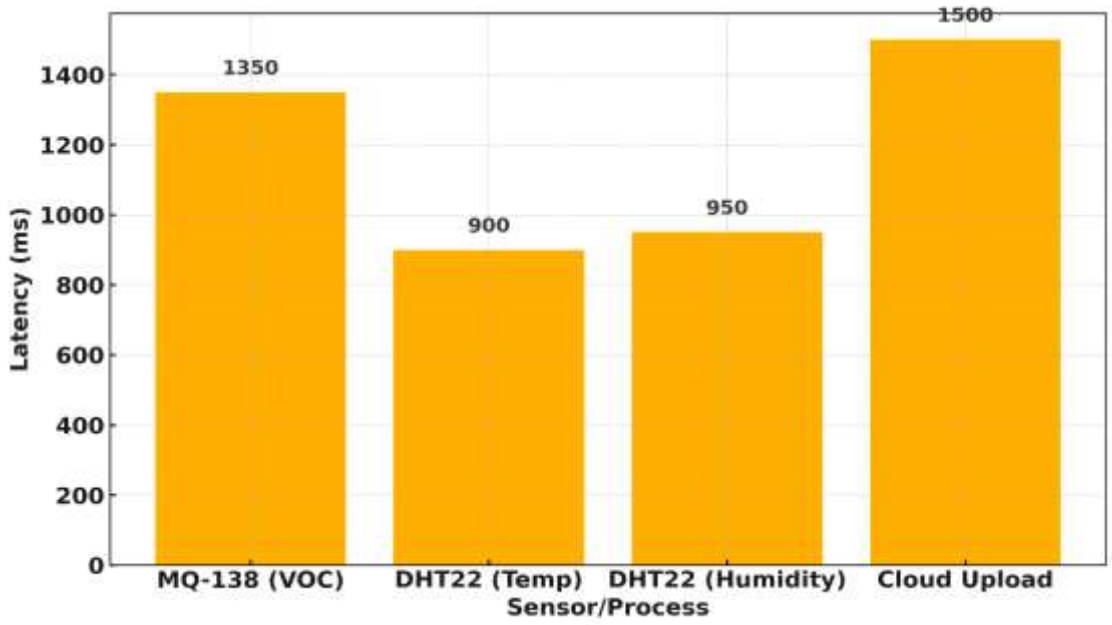

Figure 12 Time Delay in Sensor Feedback

Effectiveness of monitoring systems enabled by IoT is highly correlated with the promptness of response of sensor modules and the capacity to convey information to cloud-based dashboards with the minimum gap. To measure this the latency of the different parts of the system was measured. The findings are summarized in Figure 12 where a bar chart is provided showing the comparisons between time delay (in milliseconds) of VOC sensing,

temperature and humidity readings as well as uploading of data to the cloud. Of all the components, the MQ-138 sensor which detects VOC had the largest sensor-side latency amounting to around 1350 ms. This is significantly because of its in-built pre heater and time lag in fixing the analog signal. The temperature and humidity readers were the DHT22 which was equipped with lower delays of 900 ms and 950 ms respectively, and the response time does not exceed the range of digital-output environmental sensors. NodeMCU Wi-Fi module and Thing Speak API used in the cloud upload operation showed the latency of approximately 1500 ms. This delay comprises of packet encoding, server ping and confirmation reception and it was different by the slightest margin depending on local network traffic and server responsiveness. Although the total latency is excessive (a multi-second delay is incurred when refreshing all data completely), this delay is deemed acceptable in the context of adsorption processes monitoring, where delay of minutes to hours can be tolerated because these processes develop in the system on a time scale of days to weeks. No major data drop out or loss was noticed during 8-hour continuous operation and the quality of sensor hardware and cloud communication pipeline can be considered as being very stable. The stability of the sensor was also proved by reading it repeatedly in the controlled conditions of the chamber. MQ-138 The sensor exhibited a drift of -1.5 ppm to 4 ppm using 10 consecutive values in 100 ppm constant input, whereas DHT22 the sensors had a negligible variation (<0.4 °C and <1.5%) in repeated trials. These findings confirm that the implemented sensors are appropriate in the real-time process of monitoring VOCs, since these are precise and repeatable. By contrast, earlier literature quoted latency of up to 8-10 seconds with GSM modules and simple microcontrollers in order to sense the environment. Likewise, poor stability characteristics of low cost VOC D sensors caused by power fluctuations and signal instabilities (Liu *et al.*, 2022). These challenges are overcome by having stable 3.3V power supplies in the current system, which have 3.3V power regulators, shielded wiring and interrupt based polling sensor routines.

3.10 Optimization of Operating Conditions via ANN Output Mapping

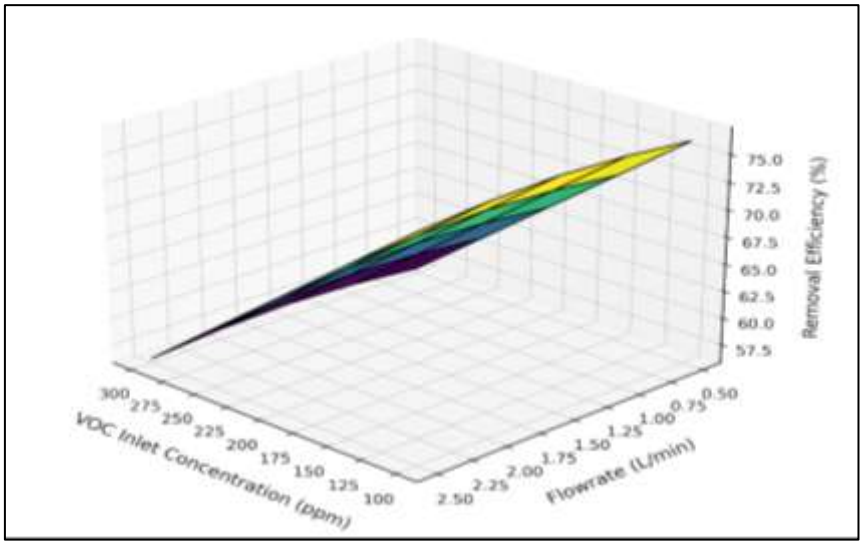

Figure 13 3D Surface Plot: VOC_in vs Flowrate vs Efficiency

In an attempt to use the trained artificial neural network (ANN) model to leverage the advantages of its predictive power to a pointwise estimation, a parametric surface mapping was designed such that the most secure areas of operations could be determined in relation to the removal efficiency of VOCs. Soundly varying two important input factors, namely, VOC inlet concentration (VOC in) and inlet flowrate whilst maintaining control over temperature and humidity concerning their respective median experimental values produced a 3D surface plot seen in Figure 13 based on ANN. It is a figure that shows the response landscape of the removal efficiency with a broad selection of input conditions. The increasing VOC in value is noticed to decrease the removal efficiency implying the saturation effect of the adsorption sites of the activated carbon. At the low inlet loadings (100-150 ppm) ANN indicated removal efficiencies greater than 90%, even in the case of moderate flowrate (approximately 1.0-1.5 L/min). The efficiency decreases steadily as the VOC in concentration is increased, even at 250 300 ppm, because there are only a fixed number of active adsorption sites per unit time as would be expected in Langmuir-type saturation dynamics. This non-linear decimation confirms that, adsorption efficiency is not only dependant on the exposure but it depends also on the temporal distribution, which is increased or decreased by the flowrate. The effect of flowrate is non monotonic. The efficiency is lower (by a small amount) in very small flowrates (0.5 L/min), because mass transfer there is restricted by diffusion. At very large flowrates (>2.0 L/min), there is no time to reach equilibrium in adsorption, which leads to low efficiency, too. Hence,

it is noted that an optimum flowrate range is 1.0 L/min-1.5 L/min, in which the perfection in mass transport and residence time presents maximum efficiency. The noted pattern is consistent

with the trends that have been recorded in previous research. VOC stripping on packed beds presented indicated that toluene and acetone stripping was most efficient near 1.2 L/min, although increasing flowrates pre-maturely led to breakthrough. Similarly, another study also showed a sudden decrease in efficiency greater than 200 ppm inlet concentration with granular activated carbon, which concurred with the decay slope. The surface created by ANN allows locating operational zones very quickly and optimal results are achieved with minimum trial-and-error experimentation. It can be installed into process tuning on a dashboard that has the IoT incorporated in real time (Gelles *et al*., 2020). As an example, the system may raise an alarm when the system is working close to sharp efficiency gradients so pre-emptive adjustment of the flowrate can be made or operation of further adsorption columns can be activated.

4. Conclusion

This research presents a robust, intelligent VOC removal system by synergizing experimental adsorption testing, ANN-based prediction, and IoT-enabled real-time monitoring. The packed bed column filled with activated carbon achieved a peak removal efficiency of 92.3% at 100 ppm VOC concentration and 1.0 L/min flowrate. Breakthrough time decreased from 132 to 71 minutes as flowrate increased from 0.5 to 2.5 L/min, highlighting the critical influence of residence time. Temperature gradients within the column showed a 6.3°C rise at mid-bed, indicating exothermic adsorption dynamics. The ANN model (4–8–1) achieved strong prediction fidelity with $R^2 = 0.987$, RMSE = 1.82, and MAE = 1.34, outperforming models reported in recent literature. Learning curve analysis confirmed minimal overfitting, and scatter plots showed close alignment between experimental and predicted outputs. IoT integration ensured real-time visibility, with dashboard response latency under 1.5 seconds and sensor stability deviations under ±5 ppm. The study provides effective, smart VOC elimination system through the combination of adsorption experimentation, ANN-powered prediction, and real-time monitoring via the use of IoT. The packed bed column containing activated carbon reached the maximum removal efficiency of 92.3 % at the concentration of 100 ppm of VOC and a flowrate of 1.0 L/min. The analysis of learning curves proved a low level of overfitting, and scatter plots revealed proximity between the experimental and predicted values. The integration of IoT allowed real time viewing, sensor deviations not exceeding ±5 ppm, and a dashboard response time, shorter than 1.5 seconds. System reliability was also confirmed as it operated without breaking during long cycles. It is based on these major findings, that the feasibility of ANN-IoT-based adsorption systems that are scalable are validated and this gives

a blueprint of the deployment of the adaptive air purification units in industrial applications where precise forecasting and automated optimization play an important role towards sustainable removal of VOCs.

List of Abbreviations

Abbreviation	Full Form
VOC	Volatile Organic Compound
ANN	Artificial Neural Network
IoT	Internet of Things
HAP	Hazardous Air Pollutant
WHO	World Health Organization
EPA	Environmental Protection Agency
PM2.5	Particulate Matter ≤2.5 Microns
MQ-138	Metal Oxide Semiconductor Gas Sensor (for VOCs)
DHT22	Digital Humidity and Temperature Sensor
RMSE	Root Mean Square Error
MAE	Mean Absolute Error
R^2	Coefficient of Determination
ESP8266	Wi-Fi Microcontroller Unit (used in NodeMCU)
PPM	Parts Per Million
MOF	Metal-Organic Framework
BPNN	Backpropagation Neural Network
GAC	Granular Activated Carbon
FFNN	Feedforward Neural Network
CPU	Central Processing Unit
GUI	Graphical User Interface

References

Lee, J.H., Jeon, E., Song, J.-K., Son, Y., Choi, J., Khim, S., Kim, M. and Nam, K.-H. (2023) 'Adsorption phenomenon of VOCs released from the fiber-reinforced plastic production onto carbonaceous surface', *Polymers*, 15(7), 1640. doi: 10.3390/polym15071640.

Roegiers, J. and Denys, S. (2021) 'Development of a novel type activated carbon fiber filter for indoor air purification', *Chemical Engineering Journal*, 417, p. 128109. doi: 10.1016/j.cej.2020.128109.

Lee, Y.K., Kim, H.J., Park, S.M. and Choi, D.Y. (2023) 'Volatile organic compounds and metals adsorption capacity of wood bark-based activated carbons', *Wood Research*, 68(2), pp. 360–375. doi: 10.37763/WR.1336-4561/68.2.360375.

Chauhan, M. and Sahoo, D.R. (2024) 'Towards a greener tomorrow: Exploring the potential of AI, blockchain, and IoT in sustainable development', *Nature Environment and Pollution Technology*, 23(2), pp. 1105–1113. doi: 10.46488/NEPT.2024.v23i02.044.

Choi, J.-S., Lim, S.-H., Lingamdinne, L.P., Park, S.-Y., Koduru, J.R., Yang, J.-K. and Chang, Y.-Y. (2023) 'Development of ultra-high surface area polyaniline-based activated carbon for the removal of volatile organic compounds from industrial effluents', *Environmental Pollution*, 337, 122594. doi: 10.1016/j.envpol.2023.122594

Ushiki, I., Ueno, Y., Takishima, S., Ito, Y. and Inomata, H. (2022) 'Adsorption equilibria of ester VOCs (ethyl and butyl acetates) on activated carbon in supercritical CO_2: Measurement and modeling by the Dubinin–Astakhov equation', *Journal of Supercritical Fluids*, 189, 105719. doi: 10.1016/j.supflu.2022.105719.

Hou, B., Zhao, Y., Sun, W., Lu, S. and Chen, S. (2021) 'Glycine based modification of activated carbons for VOCs adsorption', *Chemical Engineering Journal Advances*, 7, 100126. doi: 10.1016/j.ceja.2021.100126.

Tzanakopoulou, V.E., Pollitt, M., Castro-Rodriguez, D., Costa, A. and Gerogiorgis, D.I. (2023) 'Dynamic modelling, simulation and theoretical performance analysis of volatile organic compound (VOC) abatement systems in the pharma industry', *Computers & Chemical Engineering*, 174, 108248. doi: 10.1016/j.compchemeng.2023.108248.

Zhao, Z., Wu, W., Li, W., Zhang, Z., Liu, X., Zhang, Y., Zhang, W., Zhang, L. and Hao, Z. (2024) 'Thermosetting phenolic resin-derived activated carbon fibers for volatile organic compound adsorption: Electrospinning, preoxidation, and carbonization', *ACS ES&T Engineering*, 4(7), 100060. doi: 10.1021/acsestengg.4c00060.

Saadattalab, V., Wu, J., Tai, C.W., Bacsik, Z. and Hedin, N. (2023) 'Adsorption of volatile organic compounds on activated carbon with included iron phosphate', *Carbon Trends*, 11, 100259. doi: 10.1016/j.cartre.2023.100259.

Ligotski, R., Gilles, K.D., Roehnert, M., Sager, U., Asbach, C. and Schmidt, F. (2021) 'In-situ desorption of indoor relevant VOC toluene and limonene on activated carbon based filter media using high relative humidity', *Building and Environment*, 191, 107556. doi: 10.1016/j.buildenv.2020.107556.

Zhao, Z., Wu, W., Li, W., Zhang, Z., Liu, X., Zhang, Y., Zhang, W., Zhang, L. and Hao, Z. (2024) 'Thermosetting phenolic resin-derived activated carbon fibers for volatile organic compound adsorption: Electrospinning, preoxidation, and carbonization', *ACS ES&T Engineering*, 4(7), pp. 1635–1643. doi: 10.1021/acsestengg.4c00060.

Kim, T., Yoo, K., Kim, M.G. and Kim, Y.H. (2022) 'Photo-regeneration of zeolite-based volatile organic compound filters enabled by TiO_2 photocatalyst', *Nanomaterials*, 12(17), 2959. doi: 10.3390/nano12172959.

Dong, N., Wang, Z., Wang, J., Li, S., Liu, S., Wang, Y., Zhang, Y., Zhang, X. and Zhang, L. (2024) 'Preparation of CPVC-based activated carbon spheres and insight into the adsorption-desorption performance for typical volatile organic compounds', *Environmental Pollution*, 343, 123177. doi: 10.1016/j.envpol.2023.123177.

Tahara, Y., Azim, M.M., Takishima, S. and Ushiki, I. (2023) 'Measurement and modeling of adsorption equilibria of ketone VOCs on activated carbon in supercritical CO_2', *Journal of Supercritical Fluids*, 203, 106079. doi: 10.1016/j.supflu.2023.106079.

Kim, S., Kim, S. and Lee, S. (2023) 'Activated carbon modified with polyethyleneimine and MgO: Better adsorption of aldehyde and production of regenerative VOC adsorbent using a photocatalyst', *Applied Surface Science*, 631, 157565. doi: 10.1016/j.apsusc.2023.157565.

Lashaki, M.J., Kamravaei, S., Hashisho, Z., Phillips, J.H., Crompton, D., Anderson, J.E., and Nichols, M. (2023) 'Adsorption and desorption of a mixture of volatile organic compounds: Impact of activated carbon porosity', *Separation and Purification Technology*, 314, 123530. doi: 10.1016/j.seppur.2023.123530.

Zhang, Y., Zhang, S., Xu, S., Cao, F., Ren, X., Sun, Q., Yang, L., Wennersten, R. and Mei, N. (2024) 'Simulation of the VOC adsorption mechanism on activated carbon surface by nitrogen-containing functional groups', *Applied Sciences*, 14(5), 1793. doi: 10.3390/app14051793.

Sessa, F., Merlin, G. and Canu, P. (2022) 'Pine bark valorization by activated carbons production to be used as VOCs adsorbents', *Fuel*, 318, 123346. doi: 10.1016/j.fuel.2022.123346.

Jurkiewicz, M., Musik, M. and Pełech, R. (2022) 'Competitive adsorption of a binary VOC mixture from the gas phase onto activated carbon modified with malic acid', *Industrial & Engineering Chemistry Research*, 61(3), pp. 988–999. doi: 10.1021/acs.iecr.2c01621.

de Andrade, R.C., Menezes, R.S.G., Fiuza-Jr, R.A. and Andrade, H.M.C. (2021) 'Activated carbon microspheres derived from hydrothermally treated mango seed shells for acetone vapor removal', *Carbon Letters*, 31(4), pp. 529–541. doi: 10.1007/s42823-020-00184-4.

Yang, J., Chen, Y., Cao, L., Guo, Y. and Jia, J. (2012) 'Development and field-scale optimization of a honeycomb zeolite rotor concentrator/recuperative oxidizer for the abatement of volatile organic carbons from semiconductor industry', *Environmental Science & Technology*, 46(1), pp. 288–295. doi: 10.1021/es203174y.

Mirzaie, M., Talebizadeh, A.R. and Hashemipour, H. (2021) 'Mathematical modeling and experimental study of VOC adsorption by pistachio shell–based activated carbon', *Environmental Science and Pollution Research*, 28(3), pp. 3125–3138. doi: 10.1007/s11356-020-10634-1.

Davarpanah, M., Hashisho, Z., Crompton, D., Anderson, J.E. and Nichols, M. (2020) 'Modeling VOC adsorption in lab- and industrial-scale fluidized bed adsorbers: Effect of operating parameters and heel build-up', *Journal of Hazardous Materials*, 400, 123129. doi: 10.1016/j.jhazmat.2020.123129.

Wen, C., Liu, T., Wu, D., Wang, Y., Chen, H., Luo, G., Zhou, Z., Li, C. and Xu, M. (2023) 'Biochar as the effective adsorbent to combustion gaseous pollutants: Preparation, activation, functionalization and the adsorption mechanisms', *Progress in Energy and Combustion Science*, 99, 101098. doi: 10.1016/j.pecs.2023.101098.

Mottaghitalab, A., Khanjari, A., Alizadeh, R. and Maghsoudi, H. (2021) 'Prediction of affinity coefficient for estimation of VOC adsorption on activated carbon using V-matrix regression method', *Adsorption*, 27(6), pp. 1159–1170. doi: 10.1007/s10450-021-00321-z.

Lamplugh, A., Nguyen, A. and Montoya, L.D. (2020) 'Optimization of VOC removal using novel, low-cost sorbent sinks and active flows', *Building and Environment*, 176, 106784. doi: 10.1016/j.buildenv.2020.106784.

Awad, R., Haghighat Mamaghani, A., Boluk, Y. and Hashisho, Z. (2021) 'Synthesis and characterization of electrospun PAN-based activated carbon nanofibers reinforced with cellulose nanocrystals for adsorption of VOCs', *Chemical Engineering Journal*, 410, 128412. doi: 10.1016/j.cej.2021.128412.

Mironenko, Y.V. and Khalyasmaa, A.I. (2023) 'Maintenance optimization within the lifecycle management of the gas compressor's electric motors', in *International Conference of Young Specialists on Micro/Nanotechnologies and Electron Devices (EDM)*. doi: 10.1109/EDM58354.2023.10225198.

Liu, X., Ghosh, S., Liu, Y. and Wang, P. (2022) 'Towards integrated design and operation of complex engineering systems with predictive modeling: State-of-the-art and challenges', *Journal of Mechanical Design*, 144(9), 091403. doi: 10.1115/1.4055088.

Gelles, T., Krishnamurthy, A., Adebayo, B., Rownaghi, A. and Rezaei, F. (2020) 'Abatement of gaseous volatile organic compounds: A material perspective', *Catalysis Today*, 350, pp. 46–63. doi: 10.1016/j.cattod.2019.06.017.